Modeling and Identification of a Nonlinear SDOF Moored Structure, Part 1—Hydrodynamic Models and Algorithms

S. Narayanan
Skillings-Connolly, Inc.
5016 Lacey Boulevard S.E.
Lacey, WA 98503 USA
e-mail: chithra@skillings.com

S. C. S. Yim
Department of Civil Engineering
Oregon State University
Corvallis, OR 97331 USA
e-mail: solomon.yim@oregonstate.edu

The highly nonlinear responses of compliant ocean structures characterized by a large-geometry restoring force and coupled fluid-structure interaction excitation are of great interest to ocean and coastal engineers. Practical modeling, parameter identification, and incorporation of the inherent nonlinear dynamics in the design of these systems are essential and challenging. The general approach of a nonlinear system technique using very simple models has been presented in the literature by Bendat. In Part 1 of this two-part study, two specific nonlinear small-body hydrodynamic Morison type formulations: (A) with a relative-velocity (RV) model, and (B) with an independent flow-field (IFF) model, are formulated. Their associated nonlinear system-identification algorithms based on the reverse multiple-input/single-output (R-MI/SO) system-identification technique: (A.1) nonlinear-structure linearly damped, and (A.2) nonlinear-structure coupled hydrodynamically damped for the RV model, and (B.1) nonlinear-structure nonlinearly damped for the IFF model, are developed for a specific experimental submerged-sphere mooring system under ocean waves exhibiting such highly nonlinear response behaviors. In Part 2, using the measured input wave and output system response data, the algorithms derived based on the MI/SO linear analysis of the reverse dynamic systems are applied to identify the properties of the highly nonlinear system. Practical issues on the application of the R-MI/SO technique based on limited available experimental data are addressed. [DOI: 10.1115/1.1710875]

Introduction

Complex nonlinear responses have been observed and demonstrated in various compliant ocean systems characterized by large-geometry nonlinear mooring restoring force and coupled fluid-structure interaction exciting force [1,2]. An understanding of these nonlinear responses, including coexisting periodic *primary, subharmonic and superharmonic resonances* and aperiodic *quasi-periodic, chaotic* phenomena under both deterministic and noisy excitations, is essential to incorporate these responses in future engineering design for safe operation of these structures.

When examining the complex dynamic responses of these highly nonlinear systems, it is important to develop sophisticated analytical models that the details of the nonlinear responses can be captured accurately. However, at the same time the models have to be sufficiently simple that modern geometrical analysis techniques and efficient computer simulations can be performed. Deterministic analysis theories and numerical prediction techniques of relatively simple models have been developed to analyze the complex nonlinear phenomena for single-point mooring systems [2] ships [1], and multi-point mooring systems [3,4]. Lin and Yim [5,6] developed stochastic extensions of these techniques and corresponding analyses. They provided guidelines for interpreting field and experimental observations where randomness cannot be neglected.

To calibrate the prediction capability of these analytical techniques and simulation models, a number of experiments have been conducted [7–9]. In order to calibrate analytical predictions with experimental results, the system parameters employed in the analytical techniques need to be identified. Because the system is nonlinear, conventional system identification techniques based on linear system theory [10] are not applicable. For relatively simple nonlinear systems, however, a Reverse Multiple-Input/Single-Output (R-MI/SO) technique has been developed to determine amplitude and frequency dependent properties of some simple nonlinear systems such as the Duffing and Van der Pol types subjected to broadband excitation inputs [11]. Numerically simulated responses to random excitations were used to verify the technique.

Experiments on a single-degree-of-freedom (SDOF) nonlinear multi-point moored submerged sphere subject to wave excitations have been conducted at the O. H. Hinsdale Wave Laboratory at Oregon State University [12]. Measured results for both systems indicated that various types of nonlinear responses including harmonic, sub-harmonics, super-harmonics and chaotic responses were present.

In this study, two alternative small-body Morison type models of coupled fluid-structure interaction excitations—(A) a relative velocity (RV) model that fully couples wave motion and dynamic structural response, and (B) an independent flow-field (IFF) model that decouples the fluid and structural velocities, are formulated for the specific experimental mooring system conducted at Oregon State and their applicability examined in detail. For the RV model, a straightforward system identification algorithm (A.1)—nonlinear-structure linearly damped (NSLD) is first derived using the R-MI/SO technique. In addition, based on the concept of R-MI/SO technique, which identifies any number of nonlinear system parameters [11], an iterative version (A.2) called nonlinear-structure coupled hydrodynamically damped (NSCHD) algorithm, is derived to improve the accuracy of the identified parameters. For the IFF model, the associated algorithm (B.1) with a nonlinear-structure nonlinearly damped (NSND) assumption is derived. In Part 2, the resulting systems using the identified parameters obtained based on these three algorithms are employed to depict the responses of the fluid-structure interaction of the

Contributed by the OOAE Division for publication in the JOURNAL OF OFFSHORE MECHANICS AND ARCTIC ENGINEERING. Manuscript received July 9, 2002; final revision, September 27, 2003. Associate Editor: R. Riggs.

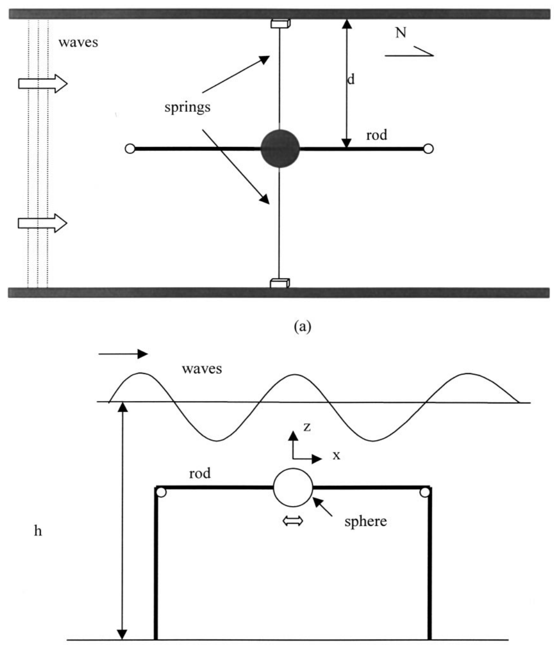

Fig. 1 SDOF experimental set up: *a*) plan, *b*) profile view

SDOF, symmetric spherical mooring system. Appropriateness and practical issues of these models and algorithms are examined in detail using experimental data.

Note that there are alternates to the use of Morison's equation for hydrodynamics forces. These include fully nonlinear potential flow and Reynolds Averaged Navier-Stokes equations to model fluid flows and pressure forces on the structural system. However, the computational efforts are much more involved, and coupled fluid-structure interaction analysis will require the use of super or parallel computers.

System Considered

The SDOF structural experimental system consists of a submerged two-point moored neutrally buoyant sphere excited by regular and random waves. Springs are attached to the sphere to provide the restoring force at an angle of 90 deg (see [4] for details). Although the mooring lines are linearly elastic, the restoring force is strongly nonlinear with large geometric stiffness. For the SDOF system, the sphere is restricted to moving only in the surge direction by passing a rigid steel rod through its center. Plan and profile views of this setup are shown in Fig. 1. Eight tests were conducted on the sphere with periodic plus band-limited white noise excitations [12]. The wave displacement and surge response of the sphere were measured and the wave velocity and acceleration were numerically evaluated using a central-difference method [13].

Governing Equation

The equations of motion for two (a relative-velocity and an independent flow-field) excitation models of the SDOF moored structural system subjected to excitations consist of periodic waves perturbed with random noise are derived in this section. The excitation force takes into account both nonlinear drag and inertia effects on a submerged symmetric small body using the Morison type model [14]. Through an appropriate transformation, the randomness in the wave field is incorporated into the hydrodynamic forcing terms.

Dynamic Equilibrium. By considering dynamic equilibrium in the surge direction, the governing equation of motion for the SDOF mooring system in standard form can be written as

$$m\ddot{x}(t)+C_s\dot{x}(t)+R(x(t))=f(t) \tag{1}$$

where m = mass of the sphere, $f(t)$ = hydrodynamic force acting on the sphere, C_s = linear structural damping coefficient, $R(x(t))$ = nonlinear restoring force, $x(t)$, $\dot{x}(t)$, $\ddot{x}(t)$ are the system displacement, velocity and acceleration, respectively. In the SDOF model, due to the presence of the rod passing through the center (used to prevent vertical (heave) and side (sway) motions, see Fig. 1), the structural damping mechanism includes a time dependent Coulomb friction component originating from the (time varying) lift force and combined drag/lift moment. As a first approximation, it is assumed here that the structural damping can be lumped into an equivalent linear structural-damping coefficient C_s. The nonlinear restoring force and excitation force are described in the following subsections.

Restoring Force. The restoring force includes an elastic force due to the mooring lines and a vertical force due to hydrostatic buoyancy. Because the sphere used for the experiment was neutrally buoyant, the forcing caused by hydrostatic buoyancy is negligible [12]. The resulting inline force $R(x(t))$ may be derived from a potential function $V(x(t))$, which describes the pretensioned geometrical configuration of a symmetric small body [4].

$$V(x(t))=K([l_1(x(t))-l_c]^2+[l_2(x(t)-l_c]^2) \tag{2a}$$

With the mooring angles attached at 90 deg, the spring lengths l_1 and l_2 can be expressed as

$$l_{1,2}=1=\sqrt{d^2+x(t)^2} \tag{2b}$$

Knowing that $R(x(t))=d/dx(V(x(t))$, the restoring force $R(x(t))$ in the surge direction is derived as given below:

$$R(x(t))=4Kx(t)\left(1-\frac{l_c}{l}\right) \tag{3a}$$

where K = spring constant, l_c = initial spring length, and d = distance of the center of the sphere from the wall (Fig. 1). The restoring force can be approximated by a high order polynomial obtained through a least square approximation. Polynomials of various orders have been employed and an optimum fit within the experimental range is identified. The polynomial can be expressed as

$$R'(x(t))\cong a_1x(t)+a_2x(t)^2+a_3x(t)^3 \tag{3b}$$

For the experimental model, a comparison of the approximate restoring force, $R'(x(t))$, in Eq. (3*a*) with the geometric model restoring force, $R(x(t)$, in Eq. (3*b*) is given in Fig. 2*a*. It can be observed that $R'(x(t))$ matches very well with $R(x(t))$. A normalized (relative) error measure, $|R(x(t))-R'(x(t))|/|R(x(t))|$, between the geometric model and approximate restoring force functions is given in Fig. 2*b*. The error is found to be negligible (much less than 1%), over the range where the restoring force is significant.

The mooring line stiffnesses are selected to provide the desired vibration frequencies and resonance motions to maximize the occurrence of nonlinear responses in the wave basin setting. The hydrodynamic forces on the mooring lines, which are piano wires, in contact with the fluid are negligible by design. The rod, which is 1-inch square steel, is practically rigid and not affected by hydrodynamic effects.

Hydrodynamic Force Models. Using linear wave theory as described in [15], the horizontal water particle velocity is given by

$$u(t)=\omega a\frac{\cosh ks}{\sinh(kh)}\cos(kx(t)-\omega t) \tag{4a}$$

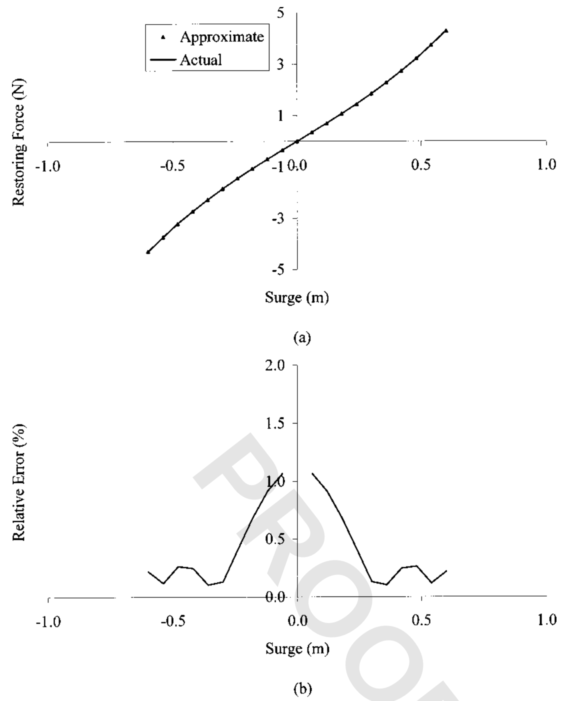

Fig. 2 Comparison between the geometric model and approximate restoring force functions: *a*) force, *b*) relative error

where u = water particle velocity in surge direction, a = dominant wave amplitude, ω = angular velocity, k = wave number, h = water depth, and s = distance of the instantaneous center of the sphere from the bottom.

The wave excitation can be considered as a randomly perturbed regular wave field. With wave elevation, $\eta(t)$, measured, Eq. (4*a*) can be approximated by

$$u(t)=\omega \frac{\cosh ks}{\sinh(kh)}\eta(t) \tag{4b}$$

It is assumed that the random perturbations in the excitation are included in $\eta(t)$, given by

$$\eta(t)=a\cos(kx(t)-\omega t+\phi)+\xi(t) \tag{4c}$$

where, in this study, $\xi(t)$ is a zero-mean delta-correlated white noise. The horizontal water particle acceleration can also be approximated as

$$\dot{u}(t)=\omega \frac{\cosh ks}{\sinh(kh)}\dot{\eta}(t) \tag{5}$$

where $\dot{u}(t)$ is the water particle acceleration in surge direction. The system diagram for the calculation of water particle velocity and acceleration from the experimental wave input is given in Fig. 3*a*.

A. Relative-Velocity Model. A relative-velocity (RV) model that couples the fluid-structure velocities can be used as one form for the Morison equation to express the forces on the sphere which are given by

$$f(t)=\rho\forall C_m\dot{u}(t)-m_a\ddot{x}(t)+\frac{\rho}{2}A_pC_d(u(t)-\dot{x}(t))|u(t)-\dot{x}(t)| \tag{6}$$

where

$$\forall=\frac{\pi}{6}D^3 \tag{7a}$$

$$A_p=\frac{\pi D^2}{4} \tag{7b}$$

$$m_a=\frac{\pi}{6}D^3C_a \tag{7c}$$

ρ = mass density, D = diameter of sphere, C_a = added mass coefficient, C_m = hydrodynamic inertia coefficient, and C_d = hydrodynamic drag coefficient. The values of C_m and C_d may be obtained from wave experiments while the coefficients C_a is derived from oscillating sphere in otherwise calm water. Also

$$C_m, C_d=f\left(\mathrm{Re}_F=\frac{v_{\mathrm{ro}}D}{\upsilon}, KC_F=\frac{v_{\mathrm{ro}}T_r}{D}\right) \tag{8a}$$

$$C_a=f\left(\mathrm{Re}_N=\frac{\dot{x}_oD}{\upsilon}, KC_N=\frac{\dot{x}_oT_o}{D}\right) \tag{8b}$$

where v_{ro} = amplitude of v_r, the relative velocity and T_r = combined period of v_r, $\dot{x}_o$ = amplitude of the structure velocity and T_o = period of oscillation of structure, υ = viscosity of the fluid, Re = Reynolds number, KC = Keulegan-Carpenter number. Note that, as in Chakrabarti [15], suffix F refers to far-field and suffix N to near field. The schematic diagram of the SDOF system with the RV model representing Eqs. (1 and 6) is given in Fig. 3*b*.

B. Independent Flow-Field Model. When a rigid body is free to move in waves, Chakrabarti [15] suggested that an independent flow-field (IFF) model might be used as an alternating form of the Morison equation. A linear superposition of two independent flow-fields separating the wave motion and the structure motion is used here, given by

$$f(t)=\rho\forall C_m\dot{u}(t)-m_a\ddot{x}(t)+\frac{\rho}{2}A_pC_du(t)|u(t)| - \frac{\rho}{2}A_pC_d'\dot{x}(t)|\dot{x}(t)| \tag{9}$$

where C_d' is the nonlinear structural damping coefficient. In this case, C_m and C_d are given by

$$C_m, C_d=f\left(\mathrm{Re}_F=\frac{u_oD}{\upsilon}, KC_F=\frac{u_oT_r}{D}\right) \tag{10}$$

where u_o = amplitude of the water particle velocity. The schematic diagram of the SDOF system using the IFF model as a form of Morison force is given in Fig. 3*c*, which delineates Eqs. (1) and (9).

Laya et al. [16] discussed the region of applicability of the RV and IFF models in terms of reduced velocity, V_R, defined by

$$V_R=\frac{u_oT_o}{D} \tag{11}$$

It is observed that for low KC and high V_R, as in the case of the experimental system considered, the IFF model may be more appropriate. Due to the lack of a comprehensive experimental study on the determination of the appropriate forms of the Morison equation (which itself is empirical) for different combinations of parameters and experimental settings, it is difficult to assess the appropriateness of the various forms of the Morison hydrodynamic force expression. However, the R-MI/SO technique can be used as a tool to determine the appropriate form of the equation best suited for the experimental system under consideration (see discussion in Part 2).

R-MI/SO Algorithms

The general identification techniques for nonlinear dynamic systems (differential equations of motions) under a stochastic setting have been presented in detail in [11]. Its novelty lies in the causality of input and output relationship and the reversibility of

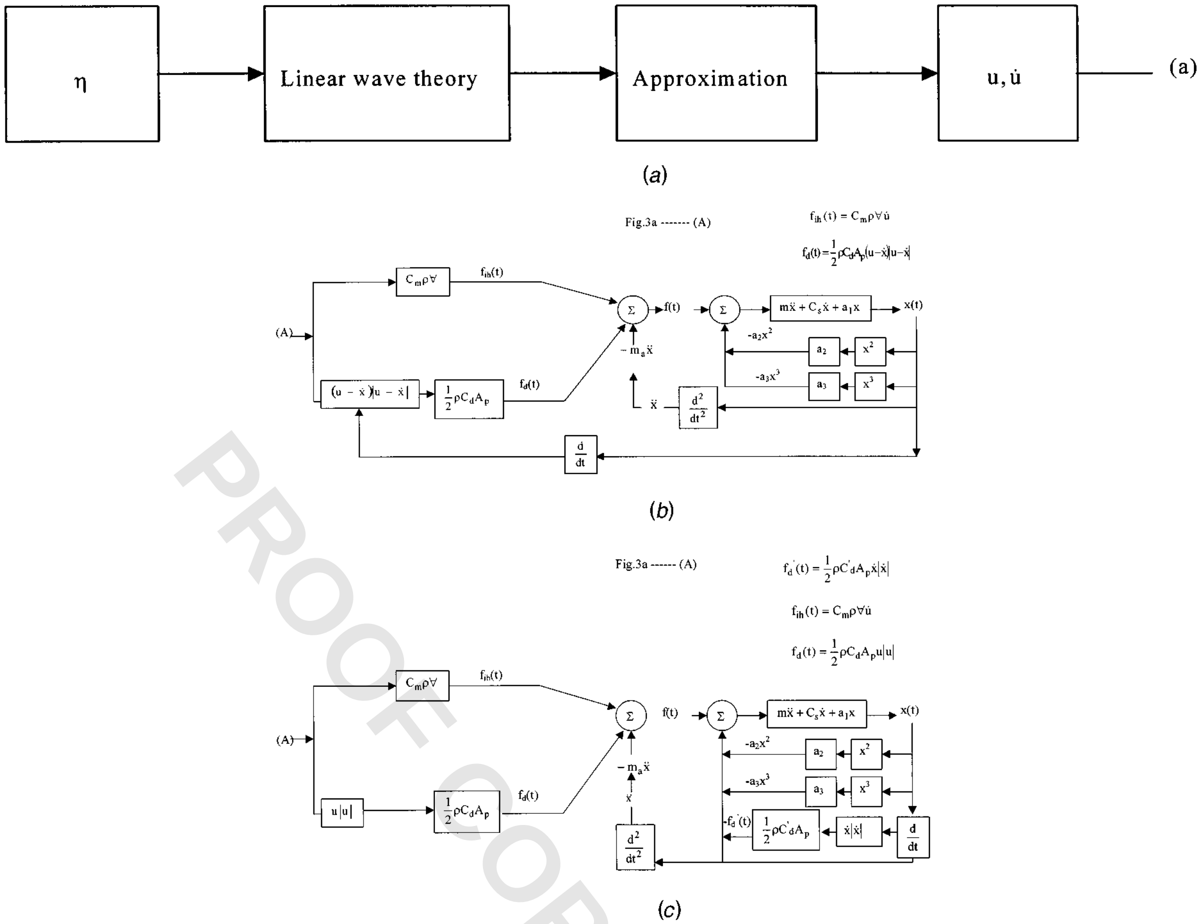

Fig. 3 Schematic diagram of the SDOF system: *a*) system diagram for the calculation of wave velocity and acceleration, *b*) RV model, *c*) IFF model

the model in terms of the input and output. While the R-MI/SO technique can be applied to most nonlinear systems subjected to random excitation irrespective of the nature of the distribution (e.g., Gaussian or non-Gaussian) of the excitation and responses [11,17], selection of the ''most appropriate'' mathematical model to represent the physical system is not straightforward. For the application of the R-MI/SO technique, depending on the availability of data and the emphasis of the modeler, many alternative algorithms can be formulated by choosing different data sets (measured and/or derived) as inputs and outputs. In general, the more measured data one has, the more sophisticated nonlinear system model one can employ. In practice, a balance between accurate physical representation and simplicity of interpretation will have to be taken into account based on the quantity and quality of available data. In this study, the hydrodynamic force, which is not measured during the experiment, is evaluated using the Morison Equation [Eqs. (6) or (9)]. With the inertia and drag force dependent on the coefficients C_m and C_d, the mathematical equation has unknown parameters (system properties as well as hydrodynamic coefficients) on both sides and applying the R-MI/SO technique to determine the system parameters need an iterative approach. Three alternative algorithms based on the RV and IFF models, with various degree of appropriateness of physical representation and simplicity, are derived and discussed below to demonstrate the level of efforts involved and the delicate balance between modeling accuracy and simplicity.

RV Algorithms. Under the relative-velocity (RV) model, the nonlinearity of the system is assumed to concentrate in the restoring force and coupled RV drag. The structural damping is assumed to be linear, or can be represented by an ''equivalent'' linear damper. The selection of this simple model allows for easy interpretation of nonlinear responses, but needs an iterative approach as one or both of the hydrodynamic coefficients need to be assumed.

A.1—Nonlinear-Structure Linearly-Damped Algorithm. Rewriting Eqs. (1), (3), and (6) using the RV model to represent hydrodynamic force, the governing equation for the nonlinear-structure linearly damped (NSLD) algorithm is

$$(m+m_a)\ddot{x}(t)+C_s\dot{x}(t)+a_1x(t)+a_2x^2(t)+a_3x^3(t)=f_a(t) \tag{12a}$$

where

$$f_a(t)=\frac{1}{2}\rho C_d\frac{\pi D^2}{4}(u(t)-\dot{x}(t))|u(t)-\dot{x}(t)|+\rho\frac{\pi}{6}D^3C_m\dot{u}(t) \tag{12b}$$

The nonlinear relative motion coupled damping is treated implicitly in the excitation force. Values of the inertia and drag coefficients, C_d and C_m, *are assumed* in order to evaluate the force f_a given by Eq. (12*b*), which is treated as the algorithm input and the system response as the algorithm output. Fourier transforming both sides of Eq. (12*a*) gives the frequency domain relation

$$(a_1+j(2\pi f)C_s-(2\pi f)^2(m+m_a))X(f)+A_2(f)X_2(f)+A_3(f)X_3(f)=F_a(f) \tag{13}$$

where

$$F_a(f)=\Im[f_a(t)] \tag{14a}$$

$$X_2(f)=\Im\lfloor x^2(t)\rfloor \tag{14b}$$

$$X_3(f)=\Im\lfloor x^3(t)\rfloor \tag{14c}$$

$$A_2(f)=a_2 \tag{14d}$$

$$A_3(f)=a_3 \tag{14e}$$

Note that the conventional symbol (dummy variable) f is used here to represent frequency in Hz in the frequency domain. Because the contact of the expressions will always be clear whether we are in time or frequency domain, it will not be confused with the same symbol representing forces in the time domain.

In the absence of nonlinear terms $x^2(t)$ and $x^3(t)$, $H(f)$ represents the frequency response function of an ideal constant parameter linear system that relates the displacement output $x(t)$ to the force input $f_a(t)$ given by

$$H(f)=\frac{X(f)}{F_a(f)}=\begin{bmatrix} a_1+j(2\pi f)C_s- \\ (2\pi f)^2(m+m_a) \end{bmatrix}^{-1}$$
$$=a_1[1-(f/f_n)^2+2\zeta_s(f/f_n)]^{-1} \tag{15}$$

where the natural frequency f_n and damping ratio ζ_s are defined, respectively, by

$$f_n=\frac{1}{2\pi}\sqrt{\frac{a_1}{(m+m_a)}} \tag{16a}$$

$$\varsigma_s=\frac{C_s}{2\sqrt{a_1(m+m_a)}} \tag{16b}$$

When the nonlinear terms are present, $H(f)$ relates the displacement output $x(t)$ to an effective force $f_e(t)$ given by

$$f_e(t)=f_a(t)-a_2x^2(t)-a_3x^3(t) \tag{17}$$

The single-input/single-output nonlinear forward algorithm with feedback, Eq. (13), is delineated in Fig. 4*a*. Identification of this system requires an iterative approach because of the presence of the feedback terms, a_2x^2 and a_3x^3, which is time-consuming. Because the forward system analysis is difficult, an alternative reverse dynamic viewpoint is considered [11]. To apply the R-MI/SO technique, the input/output roles are mathematically interchanged. This reverse dynamic system can be viewed as a three-input/single-output nonlinear algorithm without a feedback term as shown in Fig. 4*b*.

The associated Fourier transform relation is given by

$$F_a(f)=A_1(f)X_1(f)+A_2(f)X_2(f)+A_3(f)X_3(f) \tag{18}$$

where

$$X_1(f)=\Im[x_1(t)] \tag{19a}$$

$A_1(f)$, is defined as the linear impedance function which is given by

$$A_1(f)=[H(f)]^{-1}=a_1(1-(f/f_n)^2+2j\zeta_s(f/f_n)) \tag{19b}$$

Note that $x(t)$ has been replaced by $x_1(t)$ for clarity. The system gain and phase factors of Eq. (19*b*) are given by

$$|A_1(f)|=a_1[\sqrt{(1-(f/f_n)^2)^2+(2\zeta_s(f/f_n))^2}] \tag{20a}$$

$$\phi(f)=\tan^{-1}\left[\frac{2\zeta_s f/f_n}{1-(f/f_n)^2}\right] \tag{20b}$$

The minimum gain factor occurs at the resonance frequency, f_r, of the system. By maximizing Eq. (19*b*), it can be shown that for structures having damping ratio $\zeta_s\leqslant 0.5$, [18], the resonance frequency is given by

$$f_r=f_n\sqrt{1-2\zeta_s^2} \tag{20c}$$

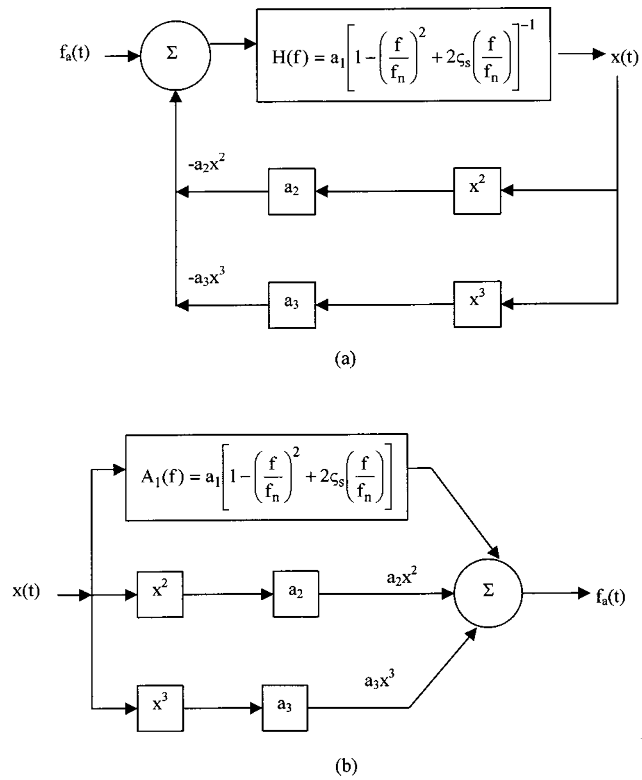

Fig. 4 The nonlinear-structure linearly damped (NSLD) algorithm: *a*) with feedback, *b*) without feedback

(A detailed explanation on how to obtain the natural vibration frequency, f_n, of the "linear system" will be presented in Part 2 using actual examples.) Hence, the minimum value of gain factor that occurs at resonance is given by

$$A_1(f_r)|=a_1\left[2\zeta_s\sqrt{1-\zeta_s^2}\right] \tag{20d}$$

For lightly damped systems, the resonance frequency, f_r, and the minimum value of the gain factor can be approximated [11] by

$$f_r\approx f_n \quad |A_1(f_r)|\approx 2a_1\zeta_s \tag{20e}$$

The physical parameters of the mooring system can therefore be estimated as follows

$$a_1\approx A_1(0) \tag{21a}$$

$$C_a=\frac{m_a}{(\pi/6\rho D^3)} \tag{21b}$$

$$C_s=2\zeta_s\sqrt{(a_1(m+m_a))}\approx\frac{|A_1(f_n)|}{2\pi f_n} \tag{21c}$$

$X_2(f)$, $X_3(f)$, $A_2(f)$ and $A_3(f)$ are given by Eq. (14). Reverse dynamic inputs $x(t)$, $x^2(t)$ and $x^3(t)$ are usually correlated. Procedures to replace the correlated inputs with a new set of uncorrelated inputs are applied to convert the nonlinear algorithm to an equivalent three-input/single-output linear algorithm [11]. The resulting impedance functions $A_1(f)$, $A_2(f)$, and $A_3(f)$ yield the three restoring force coefficients. Hence, this procedure identifies the structural damping coefficient C_s, and restoring coefficients a_1, a_2 and a_3. In performing the system identification, a sensitivity study of the identified values on the assumed values of the inertia and drag coefficients, C_d and C_m, is recommended (see Part 2).

PROOF COPY 008402JOM

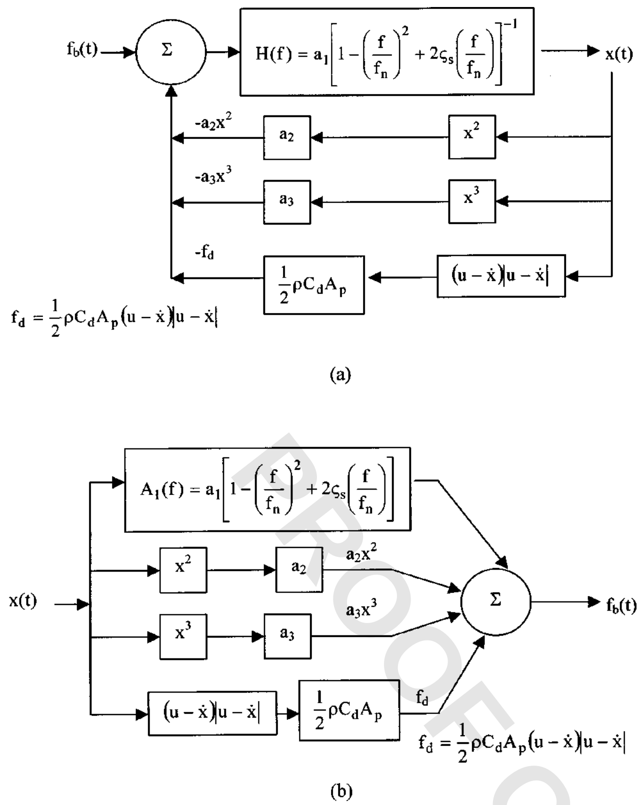

Fig. 5 The nonlinear-structure coupled hydrodynamically-damped (NSCHD) algorithm: *a*) with feedback, *b*) without feedback

A.2—Nonlinear-Structure Coupled Hydrodynamic-Damped Algorithm. When the excitation force is inertia dominated, i.e., the drag force is relatively small compared to the inertia force, a straightforward, nonlinear-structure coupled hydrodynamic-damped (NSCHD) algorithm can be derived. In this case, the nonlinear relative motion coupled damping is treated explicitly and the R-MI/SO technique is applied to identify the damping coefficient C_d along with other linear and nonlinear coefficients. The governing equation can be written as

$$(m+m_a)\ddot{x}(t)+C_s\dot{x}(t)+a_1x(t)+a_1x^2(t)+a_3x^3(t)-C_m(u(t)-\dot{x}(t))|u(t)-\dot{x}(t)|=f_b(t) \tag{22a}$$

where

$$f_b(t)=\rho\frac{\pi}{6}D^3C_m\dot{u}(t) \tag{22b}$$

This algorithm requires iterations due to the presence of the *assumed inertia coefficient*, C_m, in Eq. (22*b*). In addition, this algorithm would require a more reliable data set than the latter ones (NSLD and NSND, see below sections). Also this model can be an appropriate representation of the physical system only when the inertia force dominates.

The corresponding single-input/single-output nonlinear forward NSCHD algorithm with feedback is shown in Fig. 5*a*. The nonlinear forward algorithm is converted to a reverse dynamic algorithm by applying the R-MI/SO procedures. The corresponding reverse dynamic NSCHD algorithm without feedback is given in Fig. 5*b*.

The associated Fourier transform relation can be written as

$$A_1(f)X_1(f)+A_2(f)X_2(f)+A_3(f)X_3(f)+A_4(f)X_4(f)=F_b(f) \tag{23a}$$

where

$$X_4(f)=\Im[(u(t)-\dot{x}(t))|u(t)-\dot{x}(t)|] \tag{23b}$$

$$A_4(f)=\frac{1}{2}\rho C_d\frac{\pi D^2}{4} \tag{23c}$$

$$F_2(f)=\Im[f_2(t)] \tag{23d}$$

The frequency response functions $A_1(f)$ (described by Eqs. (19–21)), $A_2(f)$ (Eq. (14*d*)), and $A_3(f)$ (Eq. (14*e*)), identify all the system properties and $A_4(f)$ (Eq. (23*c*)) gives the hydrodynamic coefficient, C_d, in addition to the restoring force coefficients a_1, a_2 and a_3.

IFF Model Algorithm. For the IFF model, nonlinear interaction between the fluid and structural velocities is decoupled and the hydrodynamic force is evaluated using Eq. (9). Nonlinear structural damping force and the wave excitation drag force can then be treated separately.

B.1—Nonlinear-Structure Nonlinearly Damped Algorithm The IFF assumption results in the following nonlinear equation of motion (nonlinear-structure nonlinearly damped (NSND) algorithm) given by

$$(m+m_a)\ddot{x}(t)+C_s\dot{x}(t)+a_1x(t)+a_2x^2(t)+a_3x^3(t)+\rho C_d'\frac{\pi D^2}{4}\dot{x}(t)|\dot{x}(t)|=f_4(t) \tag{24a}$$

where,

$$f_4(t)=\rho\frac{\pi}{6}D^3C_m\dot{u}(t)+\rho C_d\frac{\pi D^2}{4}u(t)|u(t)| \tag{24b}$$

The NSND algorithm, which may be considered as an intermediate between the NSLD and the NSCHD algorithms, has some of the advantages of both algorithms in terms of simplicity and need for quantity and quality data. As in the NSLD case, the parameter identification for the experimental system considered needs an iterative approach as the inertia and drag coefficients, C_d and C_m, *are assumed*.

The single-input/single-output nonlinear forward algorithm with feedback is shown in Fig. 6*a*. The nonlinear forward algorithm is converted to reverse dynamic model by applying the R-MI/SO procedures. The corresponding reverse dynamic four-input/single-output nonlinear algorithm without feedback is shown in Fig. 6*b*.

The associated Fourier transform relation can be written as

$$A_1(f)X_1(f)+A_2(f)X_2(f)+A_3(f)X_3(f)+A_4'(f)X_4'(f)=F_4(f) \tag{25a}$$

where

$$X_4'(f)=\Im[\dot{x}(t)|\dot{x}(t)|] \tag{25b}$$

$$A_4'(f)=\frac{1}{2}\rho C_d'\frac{\pi D^2}{4} \tag{25c}$$

$$F_4(f)=\Im[f_4(t)] \tag{25d}$$

Using the frequency response functions $A_1(f)$ (Eqs. (19–21)), $A_2(f)$ (Eq. (14*d*)), $A_3(f)$ (Eq. (14*e*)) and $A_4'(f)$ (Eq. (25*c*)), the system properties can be identified. Thus, this procedure identifies the hydrodynamic coefficient, C_d', in addition to the restoring force coefficients a_1, a_2, and a_3.

Conclusion

The equations of motion for a SDOF submerged spherical experimental mooring system subjected to wave action for two alternate mathematical models using the small-body Morison type formulation—(A) relative-velocity (RV) model, and (B) indepen-

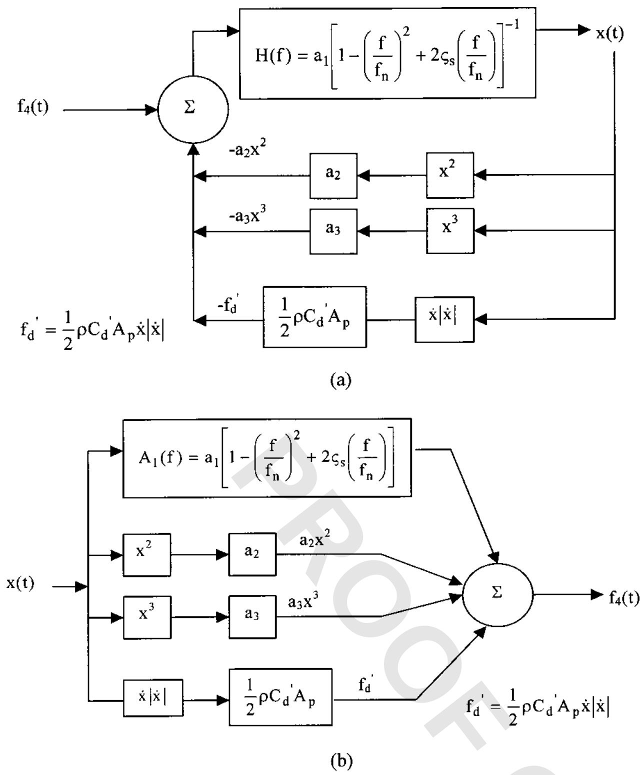

Fig. 6 The nonlinear-structure nonlinearly-damped (NSND) algorithm *a*) with feedback *b*) without feedback

dent flow-field (IFF) model, have been derived in this study. Two alternative algorithms, (A.1) nonlinear-structure coupled hydrodynamically damped (NSCHD), and (A.2) nonlinear-structure linearly damped (NSLD), for the RV model, and one, (B.1) nonlinear-structure nonlinearly damped (NSND) for the IFF model, have been developed. The nonlinear forward algorithms of these models are converted to reverse dynamic linear ones by applying the R-MI/SO technique. Details of the conversion procedures are presented and their formulations are discussed. The applicability of these mathematical models and their corresponding algorithms will be evaluated, and practical issues associated with the R-MI/SO method will discussed in Part 2 using a practical set of data from the nonlinear moored system experiment.

Acknowledgment

Financial support from the U.S. Office of Naval Research, Grant No. N00014-92-J-1221, is gratefully acknowledged.

Nomenclature

The following symbols appeared in either Parts 1 or 2 of these papers.

a = dominant wave amplitude
a_1, a_2 and a_3 = restoring force coefficients
d = distance of the center of the sphere from the wall
$f(t)$ = hydrodynamic force acting on the sphere
$f_a(t)$ = input force
$f_e(t)$ = effective force
f_n = resonance frequency of linearized system
h = water depth
k = wave number
l_c = initial spring length
l_1 and l_2 = spring lengths
m = mass of structure (sphere)
s = distance of the instantaneous center of the sphere from the bottom
u = fluid particle velocity in surge direction
$\dot{u}(t)$ = fluid particle acceleration in surge direction
u_o = amplitude of the water particle velocity
v_{ro} = amplitude of v_r
v_r, = relative velocity
$x(t)$, $\dot{x}(t)$, $\ddot{x}(t)$ = displacement, velocity and acceleration of structure as a function of time t
$\dot{x}_o$ = amplitude of the structure velocity
$A_1(f)$, $A_2(f)$ and $A_3(f)$ = Fourier transform of a_1, a_2 and a_3, respectively
C_a = added mass coefficient
C_d = hydrodynamic drag coefficient
C'_{d1} = linear structural damping coefficient
C'_d = nonlinear structural damping coefficient
C_m = hydrodynamic inertia coefficient
C_s = linear structural damping coefficient (dimensional)
D = diameter of sphere
H = high amplitude
$H(f)$ = frequency response function of an ideal constant parameter linear system
IFF = independent flow field
K = spring constant
KC = Keulegan-Carpenter number
L = low amplitude
M = medium amplitude
NSCHD = nonlinear structure coupled hydrodynamically damped
NSLD = nonlinear-structure linearly damped
NSND = nonlinear-structure nonlinearly damped
R-MI/SO = reverse multiple-input/single output
$R(x(t))$ = restoring force as a function of displacement of the structure
Re = Reynolds number
$R'(x(t))$ = approximate restoring force $R(x(t))$
RV = relative velocity
S = single-degree-of-freedom
T = wave period
T_r = combined period of v_r
T_o = period of oscillation of structure
V_R = reduced velocity
$V(x(t))$ = potential function of displacement $x(t)$
$X_1(f)$, $X_2(f)$, $X_3(f)$ = Fourier transform of x_1, x_2 and x_3, respectively
$\eta(t)$ = wave elevation
$\xi(t)$ = zero-mean delta-correlated white noise
ζ_1 = linear damping ratio
υ = viscosity of the fluid
ρ = mass density
ω = angular velocity

References

[1] Bishop, S. R., and Virgin, L. N., 1988, "The Onset of Chaotic Motions of a Moored Semi-Submersible," J. Offshore Mech. Arct. Eng., **110**, pp. 205–209.
[2] Gottlieb, O., Yim, S. C. S., and Hudspeth, R. T., 1992, "Analysis of Nonlinear Response of Articulated Tower," Int. J. Offshore Polar Eng., **2**(**1**), pp. 61–66.
[3] Bernitsas, M. M., and Chung, J. S., 1990, "Nonlinear Stability and Simulation of Two-Line Step Lowering and Mooring," Applied Ocean Research, **11**, pp. 153–166.
[4] Gottlieb, O., and Yim, S. C. S., 1993, "Drag Induced Instabilities and Chaos in Mooring Systems," *International Journal of Ocean Engineering*, **29**(6), pp. 569–599.
[5] Thompson, J. M. T., and Stewart, H. B., 1986, *Nonlinear Dynamics and Chaos*, John Wiley & Sons, Ltd, New York.
[6] Lin, H., and Yim, S. C. S., 1997, "Noisy Nonlinear Motions of a Moored System, Part I: Analysis and Simulations," J. Waterw., Port, Coastal Ocean Div., Am. Soc. Civ. Eng., **123**(**5**), pp. 287–295.
[7] Lin, H., and Yim, S. C. S., 1996, "Analysis of a Nonlinear System Exhibiting

PROOF COPY 008402JOM

Chaotic, Noisy Chaotic and Random Behaviors,'' ASME J. Appl. Mech., **63**(**2**), pp. 509–516.
[8] Isaacson, M., and Phadke, A., 1994, ''Chaotic Motion of a Nonlinearity Moored Structure,'' *Proceedings of the 4th International Offshore and Polar Engineering Conference* Vol. III, pp. 338–345.
[9] Lin, H., and Yim, S. C. S., 1998, ''Experimental Calibration of Bifurcation Superstructure of Nonlinear System,'' J. Eng. Mech. Div., **124**(**4**), pp. 471–475.
[10] Bendat, J. S., and Piersol, A. G., 1993, *Engineering Applications of Correlation and Spectral Analysis*, John Wiley & Sons, Inc., New York.
[11] Bendat, J. S., Palo, P. A., and Coppolino, R. N., 1992, ''A General Identification Technique for Nonlinear Differential Equations of Motion,'' Probab. Eng. Mech., **7**, pp. 43–61.
[12] Yim, S. C. S., Myrum, M. A., Gottlieb, O., Lin, H., and Shih, I.-M., 1993, *Summary and Preliminary Analysis of Nonlinear Oscillations in a Submerged Mooring System Experiment*, Oregon State University, Ocean Engineering Report No. OE-93-03.
[13] Gerald, G. F., and Wheatley, P. O. 1989. *Applied Numerical Analysis*, Addison-Wesley Publishing Company.
[14] Sarpkaya, T., and Isaacson, M., 1981, *Mechanics of Wave Forces on Offshore Structure*, Van Nostrand Reinhold.
[15] Chakrabarti, S. K., 1987, *Hydrodynamics of Offshore Structures*, Computational Mechanics Publications, London.
[16] Laya, E. J., Connor, J. J., and Shyam, S. Sundar, 1997, ''Hydrodynamic Forces on Flexible Offshore Structures,'' J. Eng. Mech., **123**, pp. 433–488.
[17] Bendat, J. S., 1998, *Nonlinear System Techniques and Application*, John Wiley & Sons, Inc., New York.
[18] Clough, R. W. and Penzien, J. *Dynamics of Structures*, Second Edition, McGraw-Hill, New York, 1993.

PROOF COPY 008402JOM